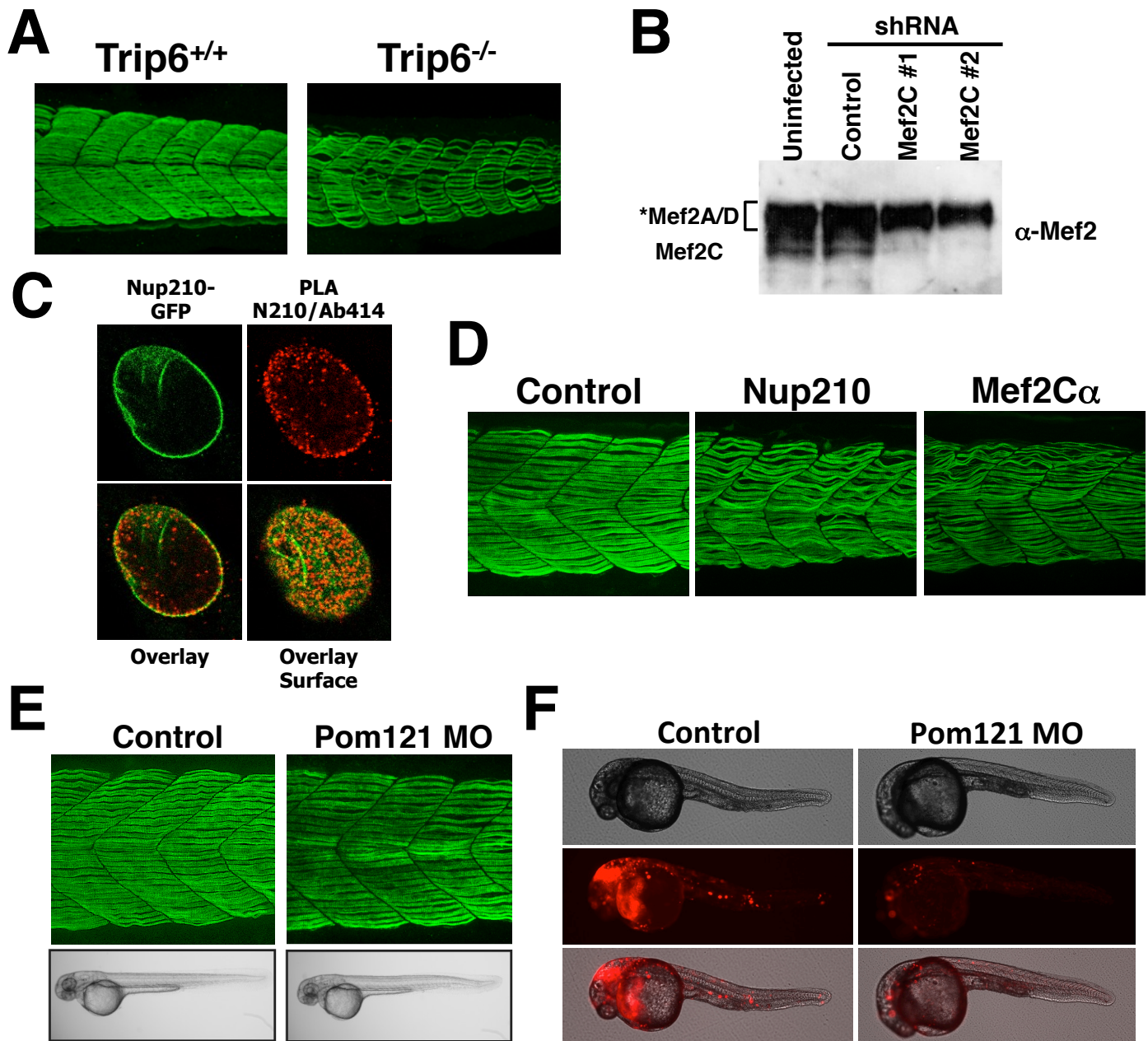


**Figure S1. Nup210 role in skeletal muscle growth. Related to Figures 1 and 2.**

(A) U2OS cells were transfected with a vector expressing V5-tagged Zebrafish Nup210. Cells were stained using the V5 antibody and the NPC antibody mAb414. Top panel shows a cross-section of the nucleus. Bottom panel shows NPCs on the nuclear surface. Zebrafish Nup210 localizes to NPCs.  $n \geq 3$  (B) Zebrafish one-cell embryos were injected with control or two different Nup210 morpholinos and slow muscle fibers were stained 48 hours post-fertilization with the F59 antibody. Representative image of a maximum projection of 30-40 sections. (C) Schematic illustration of the myogenic waves in Zebrafish based on Barresi *et al* (Barresi *et al.*, 2001). During segmentation slow muscle fibers form in the myotomes from adaxial-derived precursors (red, first myogenic wave). When segmentation is complete, at ~24 hpf, new muscle fibers form a different set of muscle precursors and are added to the dorsal and ventral side of the myotome in a process known as stratified hyperplasia (green, second myogenic wave). Sonic Hedgehog (Shh) is required for the first, but not the second, myogenic wave. Thus, the Shh inhibitor cyclopamine inhibits the formation of the early development muscle fibers (red) but not the myofibers that are added post-segmentation (green). (D) Illustration showing the experimental approach to study the role of Nup210 in post-segmentation muscle growth using cyclopamine. (E) Control or Nup210 morphants were stained 48 hpf with the slow muscle F59 antibody and the number of myofibers in myotome 20 were quantified. Bar plots represent mean  $\pm$  SEM, \*\*\*\* $p \leq 0.0001$ , two-tailed Student's t test,  $n \geq 3$  replicates. Morpholino depletions were performed with  $n \geq 50$  embryos.  $n = 10-20$  embryos from at least three independent experiments were examined by immunofluorescence and quantified.



**Figure S2. Trip6, Mef2C and Pom121 depletion in Zebrafish embryos. Related to Figures 4 and 5.**

(A) Wild-type or Trip6 CRISPR-generated mutants were stained with the F59 antibody at 48 hpf. Slow muscle was imaged by confocal microscopy. Representative image of a maximum projection of 30-40 sections.  $n \geq 10$  embryos. (B) C2C12 cells were infected at 36 hours post-differentiation with lentivirus carrying control or MEF2C-specific shRNAs. Cells were collected 72 hours post-infection and Mef2C depletion was analyzed by western blot using an anti-Mef2 antibody. According to the manufacturer anti-Mef2 recognizes Mef2A, C and D. Western blots show the specific Mef2C protein band. The specificity for Mef2A and D was not confirmed (C) The interaction of the nucleoporin Nup210 (green) with nucleoporins recognized by the mAb414 antibody, were analyzed by proximity ligation assays. PLA interactions are shown in red. (D) MEF2C $\alpha$  was depleted during Zebrafish development using specific morpholinos previously characterized (Hinits and Hughes, 2007). Slow muscle was stained at 48 hpf and compared to Control or Nup210-depleted animals. Representative image of a maximum projection of 30-40 sections.  $n = 10-20$  embryos by triplicate. (E) The transmembrane Pom121 nucleoporin was depleted during Zebrafish development and animals were analyzed at 48 hpf. No muscle alterations are observed in the absence of Pom121. Representative image of a maximum projection of 30-40 sections.  $n = 10-20$  embryos by triplicate. (F) Due to the absence of antibodies that recognize Zebrafish Pom121 we verified the effectiveness of Pom121 morpholinos by determining their ability to down-regulate the expression of a fusion RNA containing Pom121 5'UTR upstream of the RFP coding sequence as described by Veldman *et al.* Pom121 morpholinos efficiently block the translation of the fluorescent reporter ( $n = 6-10$  embryos by duplicate).

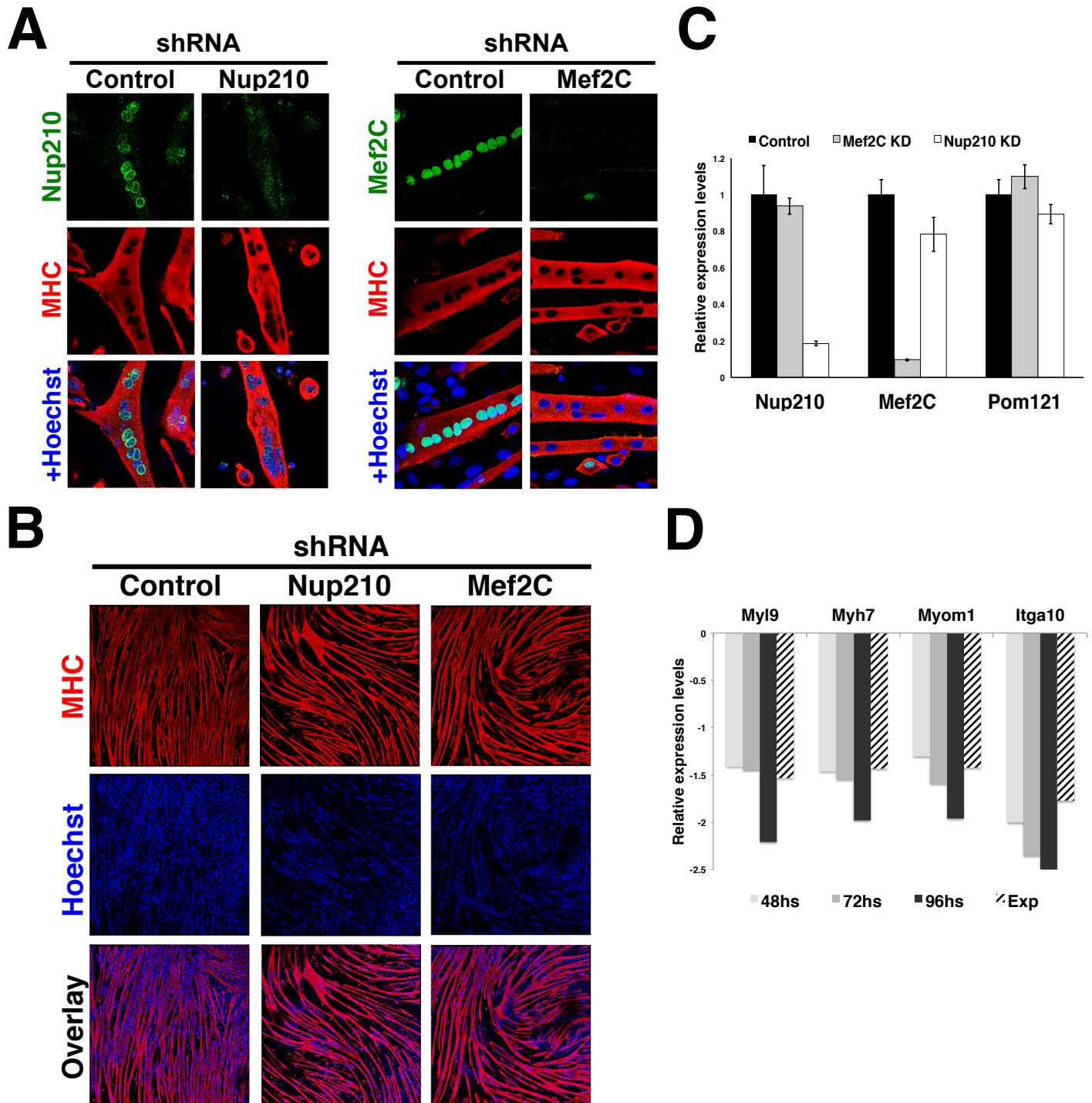


**Figure S3. Nup210 and MEF2C depletion in post-mitotic myotubes. Related to Figure 6.**

(A, B) C2C12 cells were induced to differentiate and 36 hs later were infected with lentivirus carrying Control, Nup210- and Mef2C-specific shRNAs. Cells were stained 48 hs post-infection (hpi) with Nup210, Mef2C and myosin heavy chain antibodies. (C) Total RNA was extracted from Control, Nup210, or Mef2C shRNA-treated myotubes and the expression levels of Nup210, Mef2C or the nucleoporin Pom121 were analyzed by qPCR. (D) The expression levels of several structural genes in Nup210-depleted myotubes at 48 hpi (Exp) was compared to the levels of the same genes in myotubes depleted of Nup210 at different times of depletion from (D'Angelo et al., 2012). Bar plots represent mean  $\pm$  SEM,  $n \geq 3$  replicates.

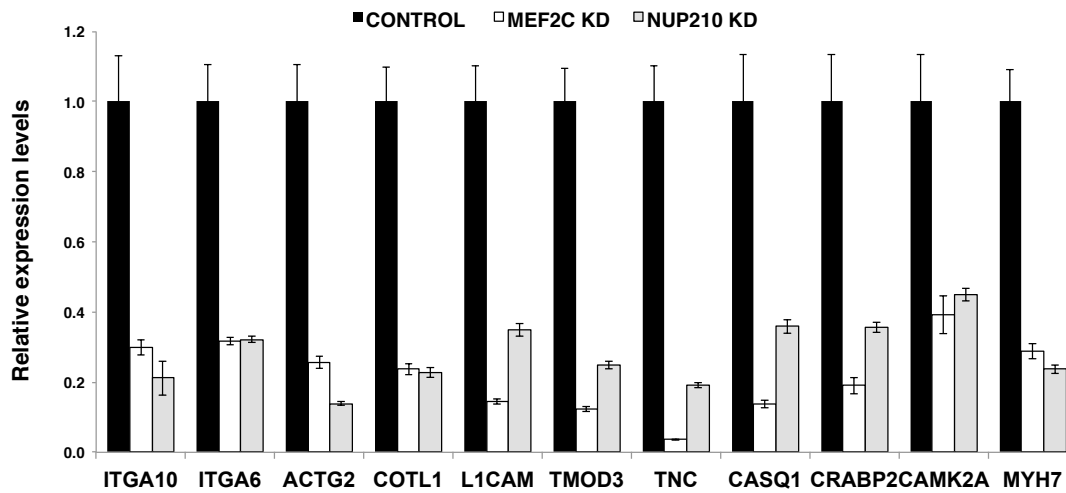


**Figure S4. Gene expression down-regulation in Nup210 and Mef2C knock-downs. Related to Figure 6.**

C2C12 cells were induced to differentiate and infected 36 hs later with lentivirus carrying Control, Nup210 and Mef2C specific shRNAs. Total RNA was collected at 48 hs post-infection and gene expression levels were analyzed by qPCR and normalized to the expression of Control cells. Bar plots represent mean  $\pm$  SEM of 3 independent experiments.



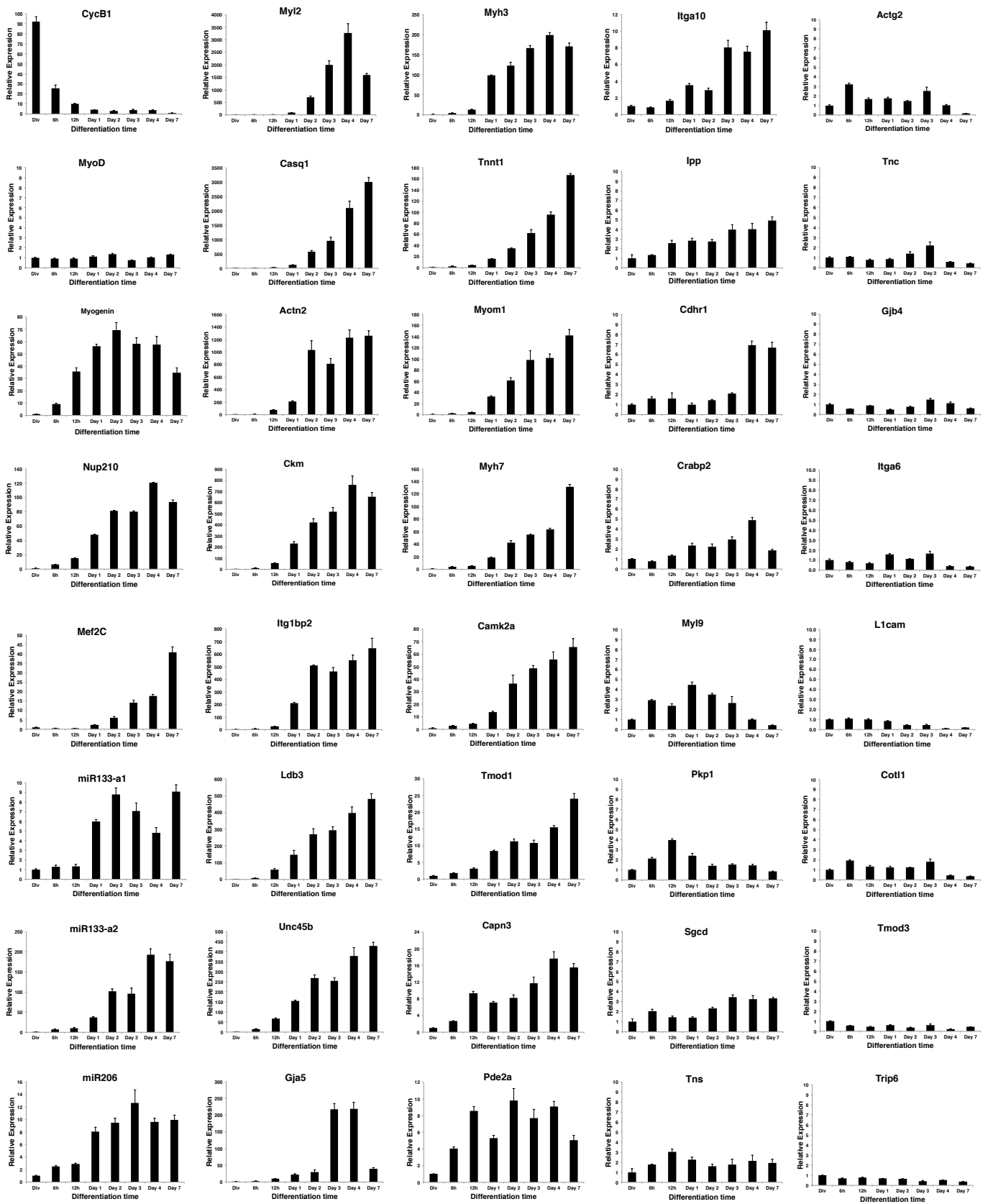


**Figure S5. Gene expression during myogenesis. Related to Figure 7.**

C2C12 cells were induced to differentiate and total RNA was collected at the indicated time points. The expression levels of genes were analyzed by qPCR, normalized to *Hprt1*, *Gapdh*, *Rr18s* and represented relative to the expression of dividing cells (Div). Cyclin B (*CycB*), *MyoD* and *Myogenin* were used as markers for differentiation. Values represent the mean of 3-5 independent experiments  $\pm$  SD. PCR primers are described in Table S5.

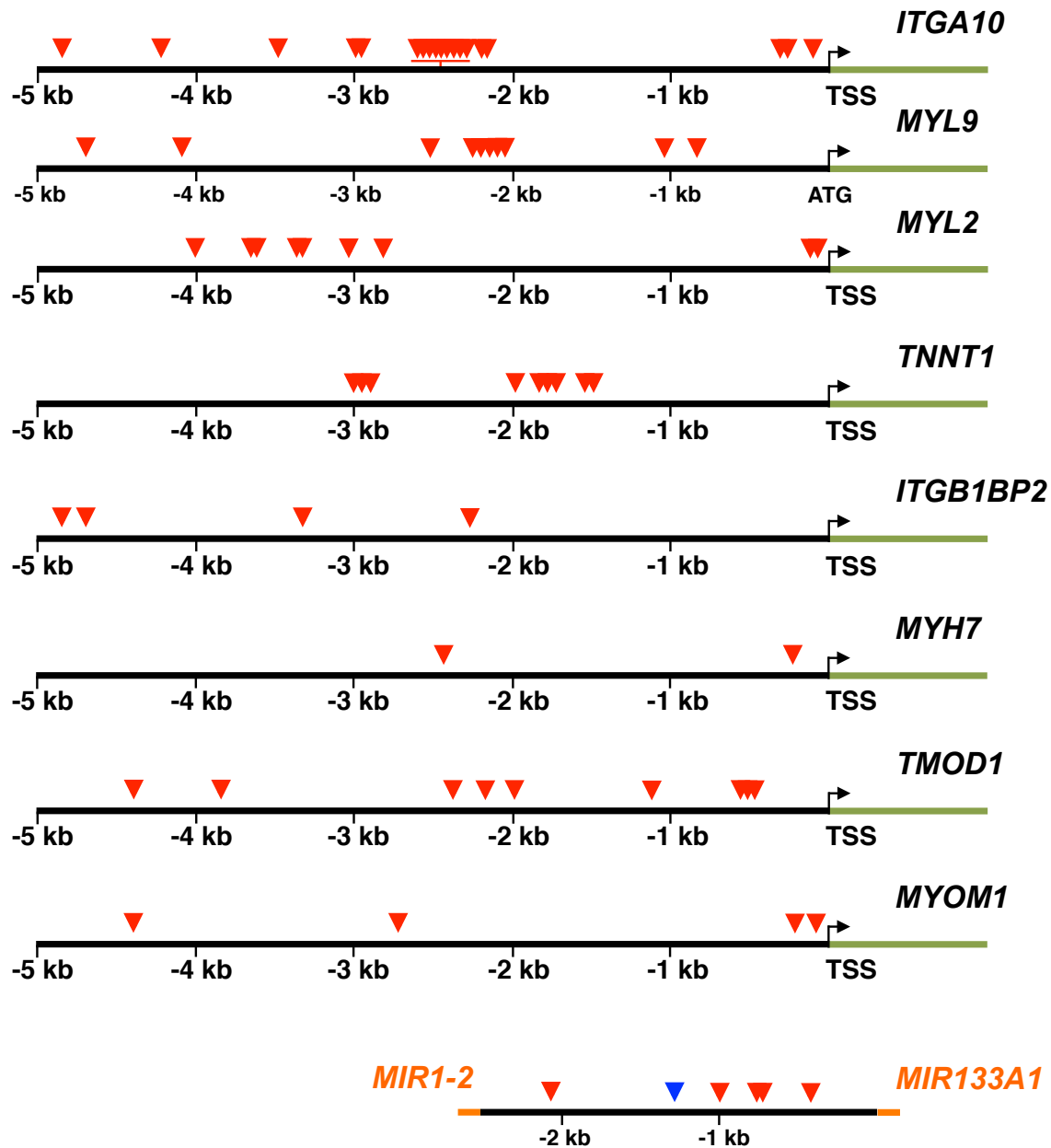


**Figure S6. Predicted Mef2C binding sites in the regulatory sequences of muscle genes. Related to Figure 7 and Table S2.**

The 5 kb sequence upstream of the transcription start site (TSS) for the indicated genes was scanned for potential Mef2C binding sites using the muscle transcription factor database of Transfact®. Red arrowheads show the approximate position of the predicted Mef2C sites (not to scale). For *MIR133A1*, the 2.5 kb sequence between this miRNA and the *MIR1-2* was scanned. Blue arrowhead shows the only confirmed Mef2C binding site (Liu et al., 2007).

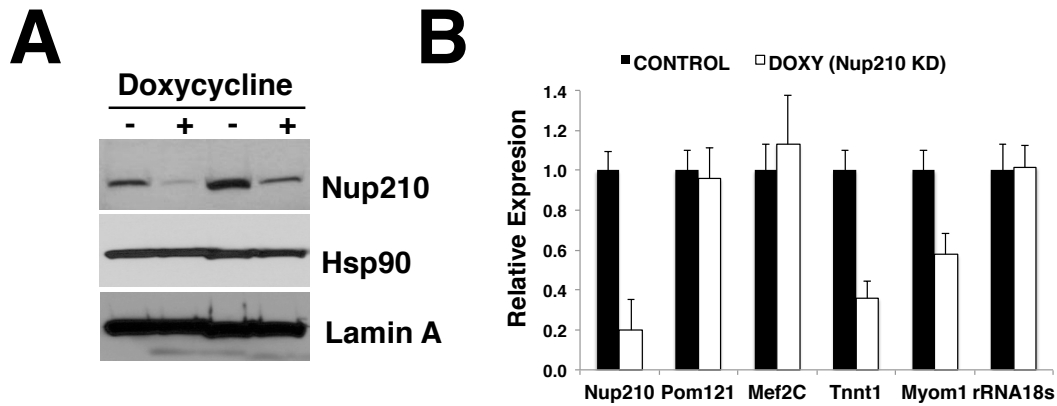


**Figure S7. Inducible shRNA dependent knock-down of Nup210 in post-mitotic myotubes. Related to Figure 7.**

(A) The C2C12 cell lines carrying a tetracycline regulated Nup210 shRNA were treated with doxycycline and Nup210 down-regulation was confirmed by western blot. Lamin A and Hsp90 were used as loading controls.  $n \geq 3$  replicates. (B) The expression levels of Nup210, Pom121, Mef2C, and the Nup210/Mef2C targets TNNT1 and MYOM1 was analyzed in the cells described in (E) by real time PCR. Bar plots represent mean  $\pm$  SEM,  $n \geq 3$  replicates.

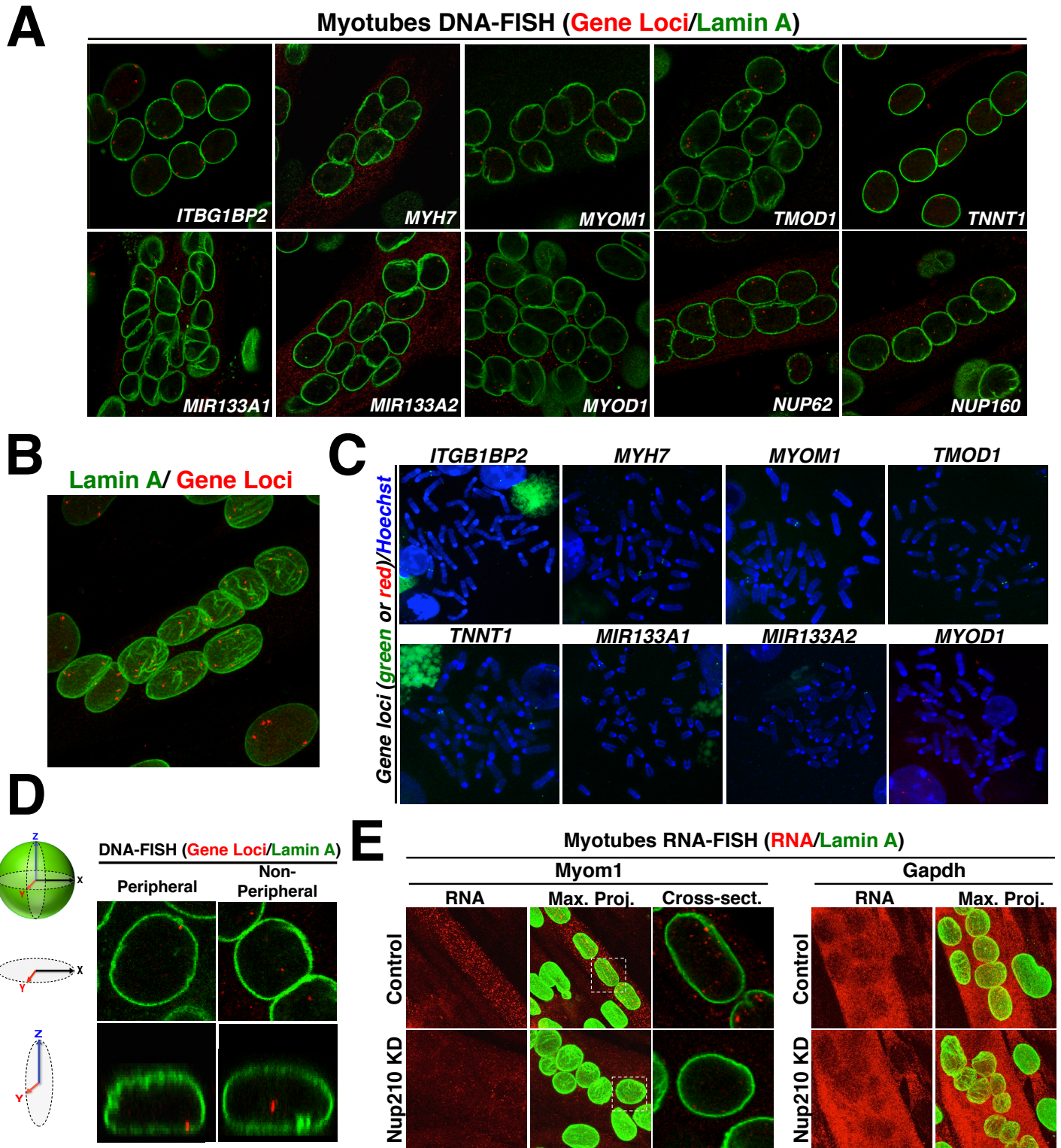


**Figure S8. Intracellular positioning of Nup210/Mef2C target genes. Related to Figure 7.**

(A) Immunofluorescence coupled to DNA-FISH was performed in post-mitotic C2C12 myotubes. Lamin A (green) gene loci (red). (B) Maximum projection of differentiated C2C12 cells labeled with the *ITGB1BP2* DNA-FISH probe showing the 4 gene copies (red), Lamin A (Green). (C) The specificity of DNA-FISH probes was determined by FISH on metaphase spreads from mouse splenocytes. Gene loci (green or red), condensed chromosomes (blue). (D) Method used to determine the association of gene loci with the nuclear envelope.  $0.3\mu\text{m}$  Z sections were used to obtain a 3D reconstructions of the nucleus and the association of genes with the nuclear periphery in the XY or ZY planes was determined. (E) RNA-FISH with Myom1 and Gapdh probes was performed in Control or Nup210-depleted myotubes. For Myom1 cross-section was performed in the plane of the strongest intranuclear foci signal. RNA (red), Lamin A (green).

Representative images of 3-5 independent experiments.



Gene	Potential MEF2C Sites	Chrom. #	Gene	Potential MEF2C Sites	Chrom. #
<i>ITGA10</i>	19	3	<i>GJA5</i>	4	3
<i>L1CAM</i>	11	X	<i>CASQ1</i>	3	1
<i>IPP</i>	11	4	<i>TMOD3</i>	3	9
<i>MYL9</i>	10	2	<i>CAMK2A</i>	3	18
<i>TNC</i>	10	4	<i>ACTG2</i>	3	6
<i>TMOD1</i>	9	4	<i>MYH7</i>	2	14
<i>TNNT1</i>	9	7	<i>ACTN2</i>	2	13
<i>MYL2</i>	9	5	<i>TNS1</i>	2	1
<i>COTL1</i>	7	8	<i>CDHR1</i>	2	14
<i>ITGA6</i>	6	2	<i>LDB3</i>	2	14
<i>MYH3</i>	5	11	<i>CRABP2</i>	1	3
<i>CAPN3</i>	5	2	<i>PKP1</i>	1	1
<i>MYOM1</i>	4	17	<i>PDE2A</i>	0	7
<i>ITGB1BP2</i>	4	X	<i>GJB4</i>	0	4
<i>CKM</i>	4	7	<i>UNC45B</i>	0	11
<i>SGCD</i>	4	11	<i>MIR133A1*</i>	6	18

**Table S2. Potential Mef2C bindings sites in Nup210/Mef2C-regulated genes. Related to Figure 7.** The 5 kb sequence upstream of the transcription start site for the indicated genes was scanned for potential Mef2C binding sites using the muscle transcription factor database of TRANSFAC®. \*For *MIR133A1* the upstream sequence that separates this miRNA from the *MIR1* gene (~2.5 kb) was scanned for MEF2C sites. This sequence has 6 predicted MEF2C binding/regulatory sites one of which has been confirmed (Liu et al., 2007).

<b>Gene</b>	<b>Gene ID</b>	<b>Morpholino name</b>	<b>Morpholino sequence (5' - 3')</b>
<i>NUP210</i>	570945	MO1	CACGAGCAGACCGACCTTCTCCATA
		MO2	CACTACTATATTTACAGGTTATGGT
<i>TRIP6</i>	792697	trip6MO1	CCAGGTGGGACCAGACATATCAGAC
		trip6MO2	CAACACACAATATAAACCATGGCAC
<i>MEF2CA</i>	30575	mef2caMO	TTTCCTTCCTCTTCCAAAAGTACAG
<i>MEF2CB</i>	798771	mef2cbMO	CCCGTCTTTTCGTCTCTCTTTCA
<i>POM121</i>	568298	pom121MO	GAAGATATCCCATAATTCCCTGCGC
<i>Control</i>		CoMO	ACCcAgCTTgTCCATACTTAgAcAT

**Table S3. Antisense morpholino oligonucleotides. Related to Figures 1-5.** All morpholinos were designed to target the 5' untranslated region region of the listed genes. Gene IDs are from the Genome Reference Consortium Zebrafish. Lowercase in Control morpholino (CoMO) depicts mismatched bases.